Analysis and Design of Multi-Phase Combined Windings for Bearingless Machines

Anvar Khamitov* Student Member, IEEE, Eric L. Severson* Member, IEEE

*Department of Electrical and Computer Engineering, University of Wisconsin-Madison, Madison, WI 53706 USA

Abstract—A multi-phase (MP) combined winding design procedure for bearingless machines is proposed and developed. Using this procedure, new bearingless motor windings can be designed and conventional motor designs with MP windings can be transformed into bearingless motors by simply modifying the phase currents. The resulting MP winding is excited by two current components - one responsible for torque creation and another for suspension force creation. By applying the appropriate Clarke transformation, independent control of force and torque can be achieved. Although there are numerous papers in the literature studying bearingless machines with MP windings and their advantages, this is the first paper to provide a formal design procedure that can be applied to any MP winding configuration. The proposed approach can be used to realize popular winding designs, including concentrated- and fractional-slot windings. The paper uses the Maxwell stress tensor to formulate the force/torque model for the MP combined winding and uses the results to derive design requirements for the MP combined winding. A sequence of winding design steps is proposed and used to design example MP combined windings.

Index Terms—Bearingless drive, bearingless motor, generalized Clarke transformation, multi-phase winding, self-bearing motor

I. INTRODUCTION

Magnetic levitation technologies have potential to replace conventional motor bearings and provide contact-free and lubricant-free support of the motor shaft. This eliminates any point of wear, bearing friction, and contamination issues. Traditionally, magnetic bearings have been used to implement magnetic levitation. However, over the past decades, bearingless motors have been developed that can simultaneously operate as a motor and magnetic bearing [1], thus, having the potential to reduce the system complexity. The radial x and y forces are typically created by a radial bearingless motor to stabilize the 2 degrees of freedom (DOF), while the other 3 DOF (tilting around x and y and displacement along z) are stabilized by another bearingless motor, magnetic bearing, or passively as in bearingless slice motors [2].

First generation bearingless machines used two separate windings to produce suspension forces and torque. In these machines, the suspension winding typically occupies an order of magnitude more slot space than is required during nominal operation in order to meet a worst-case force requirement. This leads to machine designs with decreased power density, increased ohmic and iron losses, and leakage inductance [3].

This work was supported in part by the USA National Science Foundation under Grant #1942099.

To solve these problems, several combined winding configurations have been developed, where each phase winding is responsible for both force and torque creation. Four distinct combined winding categories are found in the literature: "multiphase (MP)" [4]–[7], "dual-purpose no-voltage (DPNV)" [8]–[10], "multi-sector" [11], and "middle-point current injection" [12] windings. Of these winding types, MP and DPNV are most promising for high performance control as independent motor (torque and field weakening) and suspension (x and y forces) operation can be achieved through space vector transformations (Generalized Clarke transformation).

While the MP winding is inherently compatible with more stator designs than the DPNV winding, there is currently no generalized method that can be applied to design an MP combined winding. Study [13] provides a list of MP winding configurations and determines whether force and torque decoupling is possible. However, the results are limited to concentrated windings with one coil per phase, and no design procedure was provided to design an MP winding for an arbitrary number of slots, poles, and phases. This paper fills this gap by deriving a set of design requirements and proposing a design procedure. This work is analogous to [14], which derived design requirements and proposed a generalized design procedure for DPNV windings.

The two core contributions of the paper are:

- Determine which combinations of electric machine slots, poles, and phases can be used to design MP combined windings (Section IV).
- Propose an MP combined winding design procedure based on the star of slots approach and the results from Sections III and IV (Section V).

Section II introduces the MP combined windings and the literature about the MP systems. Section III develops a force/torque model using the Maxwell stress tensor. Using this model, MP combined windings properties, and fractional slot winding theory [15], Section IV develops design requirements in the form of constraint equations. These design requirement can also be used to determine whether existing MP motor designs can be transformed into bearingless machines through control action alone. Section V proposes an MP combined winding design procedure using star of slots approach. Finally, Section VI validates the developed theory by analyzing an example bearingless machine design with MP combined winding using finite element analysis (FEA).

II. MP COMBINED WINDINGS

It is well-known that MP machines are able to produce multiple magnetic field harmonics in the airgap [16]. Bearingless motors with MP combined windings use this capability to create one field for torque and a second field for suspension. These windings have m>3 distinct connections to the bearingless drive. Depending on the drive design requirement, the phases can be grouped to have several star connections or all phases can be connected to a single neutral point.

The phase currents in conventional MP machines can be transformed into multiple independent space vectors located in independent rotating reference frames (orthogonal subspaces) [17]. Study [18] presented a Generalized Clarke transformation matrix for symmetrical MP windings that is used to obtain these independent space vectors. In conventional MP machines, a single rotating reference frame represents the torque creation, while other reference frames represent the machine's harmonic patterns which highlight the possible unbalance among the phases [16]. A number of other studies have been presented that use these reference frames for different non-traditional purposes. Study [19], for example, presented decoupled dq axes control in multi-three-phase induction machines. Study [20] surveyed the innovative ways of exploiting additional DOFs of MP systems. One such example is series connected MP motors which are connected to a single inverter and the torque in each motor is created independently (represented by two independent space vectors).

The bearingless machine requires p pole pairs on the rotor and stator winding to create torque, and $p_s=p\pm 1$ pole pairs on the stator winding to create suspension forces. This implies that the MP combined winding must be intentionally designed to be capable of creating magnetic field harmonics at p and p_s . As a result, the same theory that is used in MP machines can be extended to MP combined windings to independently control radial suspension forces and torque in two independent rotating frames. However, the following two requirements must be met to ensure that the winding is:

- 1) symmetric a rotating magnetic field is created when supplied from a symmetrical supply.
- 2) capable of independently controlling force and torque.

The winding layout and the current excitation must be studied and used to derive these requirements in terms of the machine parameters (number of phases m, torque p and suspension p_s pole pairs, and slots Q). For this, the bearingless machine force/torque matrix model is presented in the following section and used in later sections.

III. MP COMBINED WINDING MATRIX MODEL

This section presents a bearingless machine matrix model and develops analytic expressions for the created forces and torque in terms of the phase currents and the rotor angle.

A. Force/Torque Matrix Model

The operating theory for a bearingless machine can be represented using matrices as presented in [2] and [21]. This model shows the relationship between the created forces/torque, the

drive terminal currents, and the rotor position. For a centered rotor position, this relationship can be expressed as

$$F(\theta_m) = T_m(\theta_m)i \tag{1}$$

where θ_m is a mechanical rotor angle and T_m is a matrix used to map the phase currents i into the forces and torque $F = [F_x F_y \tau]^T$ they produce on the rotor. This model holds for the surface-mounted PM motors where the quadratic relationship between the forces/torque and the phase currents is usually negligible. For a machine with m phases, T_m is of the form:

$$\boldsymbol{T_m} = \begin{bmatrix} \boldsymbol{T_{mx}} \\ \boldsymbol{T_{my}} \\ \boldsymbol{T_{mt}} \end{bmatrix} = \begin{bmatrix} T_{mx,1} & T_{mx,2} & \dots & T_{mx,m} \\ T_{my,1} & T_{my,2} & \dots & T_{my,m} \\ T_{mt,1} & T_{mt,2} & \dots & T_{mt,m} \end{bmatrix}$$
(2)

Having the phase currents $i = [i_1 \ i_2 \dots i_m]^T$ and using (2), the model (1) can be rewritten for each force and torque as

$$F_d(\theta) = \mathbf{T_{md}} \mathbf{i} = \sum_{k=1}^m F_{d,k}(\theta) = \sum_{k=1}^m T_{md,k}(\theta) i_k$$
 (3)

$$\tau(\theta) = \mathbf{T_{mt}} \mathbf{i} = \sum_{k=1}^{m} \tau_k(\theta) = \sum_{k=1}^{m} T_{mt,k}(\theta) i_k$$
 (4)

where d=x or y, and $\theta=p\theta_m$ is an electrical rotor angle. $F_{d,k}$ and τ_k are the force and torque created by phase winding k. Each T_m matrix entry can be interpreted as a per ampere force or torque created when only a single phase is excited.

Suppose that the phase currents can be written as the sum of two current vectors for suspension i_s and for torque i_t :

$$i = \begin{bmatrix} i_1 \\ i_2 \\ \dots \\ i_m \end{bmatrix} = i_s + i_t = \begin{bmatrix} i_{s,1} \\ i_{s,2} \\ \dots \\ i_{s,m} \end{bmatrix} + \begin{bmatrix} i_{t,1} \\ i_{t,2} \\ \dots \\ i_{t,m} \end{bmatrix}$$
(5)

Substituting (5) into (3)-(4), the design requirements requirements presented in Section II can be rewritten as: 1) symmetry: $T_{md}i_s$ and $T_{mt}i_t$ are independent of the rotor angle θ , and 2) independent force and torque creation: $T_{md}i_t=0$ and $T_{mt}i_s=0$. Depending on T_m matrix, the desired i_s and i_t satisfying these constraints can be determined and the MP combined winding design requirements can be derived. The derivation of the entries of T_m is now presented.

B. Derivation of T_m matrix entries

The Maxwell stress tensor is used to calculate force/torque:

$$\vec{\sigma} = \begin{bmatrix} \sigma_{\rm n} \\ \sigma_{\rm tan} \end{bmatrix} = \begin{bmatrix} \frac{1}{2\mu_0} (B_{\rm n}^2 - B_{\rm tan}^2) \\ \frac{1}{\mu_0} B_{\rm n} B_{\rm tan} \end{bmatrix} \tag{6}$$

where σ_n and σ_{tan} are the normal and tangential components of the per unit area force (stress) acting on the surface of the rotor. This force is created from the interaction between the tangential (B_{tan}) and normal (B_n) components of the magnetic field in the airgap, which are depicted in Fig. 1a. These stresses can be integrated over the rotor's airgap surface S to determine the net forces and torque acting on the rotor:

$$F_x = \int_S \vec{\sigma} \cdot \hat{\mathbf{x}} \, \mathrm{d}S, \ F_y = \int_S \vec{\sigma} \cdot \hat{\mathbf{y}} \, \mathrm{d}S, \ \tau = \int_S \vec{r} \times \vec{\sigma} \, \mathrm{d}S \quad (7)$$

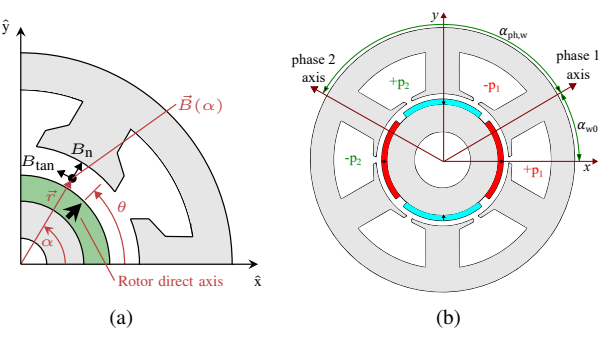


Fig. 1. Definitions of: (a) magnetic field components, unit vectors, and angles $(\alpha \text{ and } \theta)$ and (b) axes and winding phase angles $(\alpha_{\text{ph,w}} \text{ and } \alpha_{\text{w0}})$; $+p_1$ and $-p_1$ denote phase 1 coil sides going into and out of the page, respectively.

where α is the airgap angle (see Fig. 1a), \vec{r} is the airgap radius vector, and $\hat{\mathbf{x}}$ and $\hat{\mathbf{y}}$ are the unit vectors.

The T_m matrix entries are now determined using the following steps. When phase k is excited by current i_k ,

- 1) expressions for the airgap magnetic field normal $B_{n,k}$ and tangential $B_{tan,k}$ components are determined;
- 2) $F_{x,k}$, $F_{y,k}$, τ_k are determined using (7); and
- 3) finally, the T_m matrix entries are calculated from $T_{mx,k} = F_{x,k}/i_k$, $T_{my,k} = F_{y,k}/i_k$, and $T_{mt,k} = \tau_k/i_k$.

As will be shown, each T_m matrix entry is a function of the fixed machine parameters and the rotor angle, but not the phase currents. The above steps are now illustrated.

1) Step 1: The magnetic fields in the airgap are created by the rotor magnets and the stator winding currents. The field created by the magnet can be expressed as:

$$B_{\delta} = \sum_{h=1}^{\infty} \hat{B}_{\delta,h} \cos(h\alpha - \theta)$$
 (8)

where h is a spatial harmonic order and $\hat{B}_{\delta,h}$ is a corresponding amplitude. The main field harmonic that contributes to the torque creation is h = p with an amplitude \hat{B}_{δ} . This is referred to as the machine's magnetic loading [15], [22].

The field from each phase winding can be determined using the linear current density $A_k(\alpha)$ (shows the current distribution along the inner bore of the stator), which can be expressed as the sum of many sinusoidally distributed windings:

$$A_k(\alpha) = \frac{i_k}{r} \sum_{h=1}^{\infty} A'_{c,\text{ph},h} \sin\left(h[\alpha - \alpha_{\text{w},k}]\right)$$
 (9)

where $A'_{c,\mathrm{ph},h}=\frac{2}{\pi}z_Qz_c\hat{k}_{w,h}$ is a normalized parameter showing the effective number of turns per radian for the harmonic h. Here, z_Q is the number of series turns per coil, z_c is the number of coils in a phase, and $k_{w,h}$ is a harmonic h winding factor. For torque and suspension, this parameter is denoted as $A'_{c,\mathrm{ph},t}$ and $A'_{c,\mathrm{ph},s}$. The angle $\alpha_{\mathrm{w},k}$ in (9) is:

$$\alpha_{w,k} = \alpha_{w0,h}/h + [(k-1)\alpha_{ph,w}]$$
 (10)

where $\alpha_{w0,h}$ is a phase shift angle for each harmonic h. At fundamental harmonic (h = 1), $\alpha_{w0,1} = \alpha_{w0}$ is an angle

between the phase 1 axis and x axis; $\alpha_{ph,w}$ is an angle between adjacent phases, as shown in Fig. 1b.

Using (9), the winding magnetic field components created by a phase k can be determined as

$$B_{\text{n,w,}k} = \frac{\mu_0 i_k}{\delta_{\text{eff}}} \sum_{h=1}^{\infty} \frac{A'_{c,\text{ph},h}}{h} \cos\left(h[\alpha - \alpha_{\text{w},k}]\right)$$
(11)

$$B_{\text{tan,w},k} = -\frac{\mu_0 i_k}{r} \sum_{h=1}^{\infty} A'_{c,\text{ph},h} \sin\left(h[\alpha - \alpha_{\text{w},k}]\right)$$
(12)

where δ_{eff} is an effective airgap length. Using the results (8) and (11)-(12), the net normal and tangential magnetic field components in the airgap can be determined as:

$$B_{n,k} = B_{\delta} + B_{n,w,k}, \ B_{tan,k} = B_{tan,w,k}$$
 (13)

2) Steps 2 and 3: The forces and torque $F_{x,k}$, $F_{y,k}$, τ_k created by phase k current are determined using (7). The torque per phase τ_k is calculated by substituting (6) into (7):

$$\tau_k = \frac{r^2 L}{\mu_0} \int_0^{2\pi} B_{\mathbf{n},k} B_{\tan,k} \, \mathrm{d}\alpha \tag{14}$$

Evaluating (14) for harmonic p and dividing the result by i_k , entries of T_{mt} are obtained:

$$T_{mt,k} = -\hat{T}_{mt}\sin\left(\theta - p\alpha_{w,k}\right), \ \hat{T}_{mt} = \frac{V_r \hat{B}_{\delta} A'_{c,ph,t}}{r}$$
 (15)

where $V_r = \pi r^2 L$ is the rotor volume.

 T_{md} entries can be derived similarly. The difference from torque creation is that the force is created from the interaction between each harmonic h of the rotor magnetic field and harmonics $h \pm 1$ of the winding magnetic field. At rotor harmonic p, it can be shown that T_{md} entries are:

$$T_{md,k} = \hat{T}_{mf,h_1} f_d(\theta - h_1 \alpha_{w,k}) \pm \hat{T}_{mf,h_2} f_d(\theta - h_2 \alpha_{w,k})$$
(16)

where $h_1 = p - 1$ and $h_2 = p + 1$ are the winding harmonics that contribute to the force creation; the \pm term is + for d = x and - for d = y; f_x and f_y are cosine and sine functions. \hat{T}_{mf,h_1} and \hat{T}_{mf,h_s} are (17), where $p_s = h_1$ or h_2 .

$$\hat{T}_{mf,p_s} = \frac{V_r \hat{B}_{\delta} A'_{c,\mathsf{ph},h_1}}{2r} \left(\frac{1}{p_s \delta} + \frac{p_s - p}{r} \right) \tag{17}$$

The following section will use the results (15)-(16) and (3)-(4) to derive conditions for viable windings.

IV. MP COMBINED WINDING DESIGN REQUIREMENTS

MP combined windings must satisfy symmetry and independent force/torque creation requirements. This section determines which combinations of electric machine slots Q, poles p and p_s , and phases m can be used to design an MP machine that meets these requirements. The key terminology is presented in Section IV-A and an effective number of torque and suspension phases are introduced in Section IV-B. Using results from Section III, Section IV-B, and fractional slot winding theory [15], the design requirements are derived as constraint equations in Sections IV-C and IV-D. The results are summarized later, in Table I. Finally, Section IV-E compares the MP and DPNV winding design requirements [14].

A. Key Terminology

It is common practice to design conventional stator windings (non-bearingless) using the "star of slots" diagram [15]. This diagram shows the phasor of a particular harmonic of back-EMF induced in each coil side. Using this diagram, the winding layout of the motor (phase assignment to the coil sides) can be determined. This approach can be analogously extended to MP combined windings, the key difference being that two winding harmonics are now considered, h=p (torque) and $h=p_s$ (force creation). This paper uses the terms "torque star of slots" and "suspension star of slots" to indicate that the star of slots diagram is drawn at harmonic p or p_s .

Example torque and suspension star of slots diagrams are shown in Fig. 2 for a motor with $Q=8,\ p=2,$ and $p_s=3.$ The phasor of the first slot is drawn horizontally and the subsequent phasors lag by $p\alpha_u$ (or $p_s\alpha_u$). Here, $\alpha_u=2\pi/Q$ is an angle between adjacent slots in mechanical radians. Depending on the values of p and p_s , Fig. 2 shows that several slots can have the same phasor location. Furthermore, the angle between the phasors of adjacent slots may not be equal to the angle between adjacent phasors. For example, Fig. 2b shows that the angle between slots 1 and 2 is 135° , while the angle between adjacent phasors (slots 1 and 4) is 45° . This phasor angle can be determined using the following equation [15]:

$$\alpha_z = \frac{2\pi}{Q}t\tag{18}$$

where t is either gcd(Q, p) or $gcd(Q, p_s)$. This angle is later used to derive symmetry requirements.

B. Effective number of phases

This subsection introduces the notion of an "effective" number of torque and suspension phases in the MP combined winding. This concept is used later to derive symmetry requirements. In conventional MP windings, the angle $\alpha_{\rm ph,w}$ (see Fig. 1) is translated to $p\alpha_{\rm ph,w}$ in the star of slots. The angle $\alpha_{\rm ph,w}$ is selected to ensure that $p\alpha_{\rm ph,w}$ can be reduced to $2\pi/m$. In MP combined windings, the angle $\alpha_{\rm ph,w}$ corresponds to the angles α_t , α_s in the torque, suspension star of slots. These angles are not necessarily $2\pi/m$ and can be expressed as

$$\alpha_t = k_1 \frac{2\pi}{m}, \ \alpha_s = k_2 \frac{2\pi}{m} \tag{19}$$

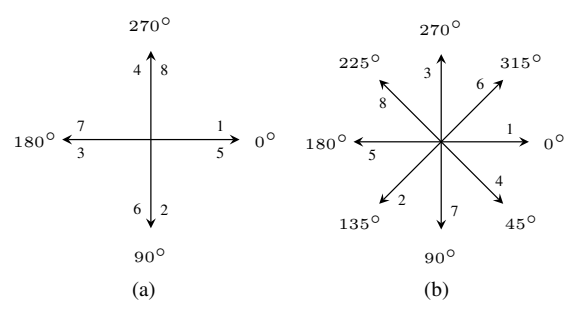


Fig. 2. Demonstration of star of slots diagrams for $Q=8,\ p=2,$ and $p_s=3$: (a) torque star of slots and (b) suspension star of slots.

where k_1 and k_2 are integer numbers. In mechanical radians, it must be true that $\alpha_{\rm ph,w}=\alpha_t/p=\alpha_s/p_s$. Substituting (19) into this expression, it can be shown that $k_1/k_2=p/p_s$. Since, p and p_s are co-prime, it must be true that $k_1=cp$ and $k_2=cp_s$, where c is an integer number. Picking the smallest positive values of $k_1=p$ and $k_2=p_s$, the phase separation angles for MP combined windings become:

$$\alpha_{\text{ph,w}} = \frac{2\pi}{m}, \ \alpha_t = p\frac{2\pi}{m}, \ \alpha_s = p_s\frac{2\pi}{m}$$
 (20)

This shows that $\alpha_{\rm ph,w}$ in MP combined windings must be constrained to $2\pi/m$. From this result, the following two observations can be drawn about MP combined windings:

- 1) The phases adjacent in the stator winding may not be adjacent in torque or suspension star of slots: For example, with p=3 and m=4, $\alpha_t=\frac{3\pi}{2}$ and the torque phases in the star of slots have angles in the order of $0, \frac{3\pi}{2}, \pi, \frac{\pi}{2}$ instead of $0, \frac{\pi}{2}, \pi, \frac{3\pi}{2}$.
- 2) The effective number of phases for torque or suspension creation can be less than m: This is true if $\gcd(m,p)>1$ or $\gcd(m,p_s)>1$. For example, for a motor with $m=8,\ p=6,\$ and $p_s=7,\ \alpha_t=3\cdot\frac{360^\circ}{4}$ and $\alpha_s=7\cdot\frac{360^\circ}{8}$. These angles show that the number of distinct phases is 4 for torque and 8 for suspension. Generally, for any MP combined winding, the distinct number of torque and suspension phases can similarly be calculated by reducing the fractions p/m or p_s/m until the numerator and the denominator are co-prime. The resulting denominator is the effective number of phases. Mathematically, defining these phases as m_t for torque and m_s for suspension, the expressions are given as

$$m_t = \frac{m}{\gcd(m, p)}, \ m_s = \frac{m}{\gcd(m, p_s)}$$
 (21)

The m_t and m_s phase numbers determine the spacing between phases in the torque and suspension star of slots:

$$\alpha_{\mathrm{ph},t} = \frac{2\pi}{m_t}, \ \alpha_{\mathrm{ph},s} = \frac{2\pi}{m_s} \tag{22}$$

The distinction between α_t and $\alpha_{\text{ph},t}$ (or α_s and $\alpha_{\text{ph},s}$) is similar to the discussion in Section IV-A, where the phasor angle α_z is analogous to $\alpha_{\text{ph},t}$ (or $\alpha_{\text{ph},s}$), while the slot angles in star of slots $p\alpha_u$ and $p_s\alpha_u$ are analogous to α_t and α_s . Note that these angles are also apparent in the phase currents, which will have a phase spacing of $\alpha_{\text{ph},t}$ for torque i_t and $\alpha_{\text{ph},s}$ for suspension i_s . However, the order that phase currents appear in a vector is based on α_t for torque and α_s for suspension.

If the number of drive connections is even, the system is called "non-reduced" (non-loaded star configuration) [15, Ch 2.9.1]. Because the star of slots will have pairs of phasors 180° apart, the phase system can be "reduced" by decreasing the original number of phases by half. If the new number of phases (after reduction) is even, a neutral point needs to be loaded. In MP combined windings, reducing the system is not possible because two phases that are 180° apart in the torque star of slots are $180^{\circ}p_s/p \neq 180^{\circ}$ apart in the suspension star of slots. Therefore, m in the following derivations denotes the number of the drive connections of a non-reduced system rather than the number of torque or suspension phases.

C. Symmetry Requirements

Symmetry requirements ensure that a rotating magnetic field is created when the winding is fed from a symmetrical supply. The MP combined winding must meet the two standard requirements (typically considered for conventional machines [15]) and new requirements, which are now presented.

1) Rotating field requirements: The first requirement is that the number of coils per phase (z_c/m) must be an integer [15]. This is listed in column 2 of Table I, where z_c is found as

$$z_c = \begin{cases} Q/2, & \text{single-layer winding} \\ Q, & \text{double-layer winding} \end{cases}$$
 (23)

The second requirement ensures that the phase spacing $\alpha_{\rm ph}=2\pi/m$ in the torque star of slots is an integer multiple of the phasor angle α_z in (18). In an MP combined winding, this is analogously extended for both torque and suspension:

$$\frac{\alpha_{\text{ph},t}}{\alpha_z} \in \mathbb{N}, \ \frac{\alpha_{\text{ph},s}}{\alpha_{zs}} \in \mathbb{N}$$
 (24)

where α_{zs} is analogous to α_z , but calculated with $h = p_s$. Substituting (18) and (22), the requirements are rewritten as

$$\frac{Q}{m}\frac{\gcd(m,p)}{\gcd(Q,p)} \in \mathbb{N}, \ \frac{Q}{m}\frac{\gcd(m,p_s)}{\gcd(Q,p_s)} \in \mathbb{N}$$
 (25)

Since $Q/m \in \mathbb{N}$, it is also true that $\gcd(Q,p)/\gcd(m,p) \in \mathbb{N}$: $\gcd(Q,p) = b\gcd(m,p)$, where $b \in \mathbb{N}$. It can be shown that Q/m is a multiple of b. This means the requirement $Q/m \cdot \gcd(m,p)/\gcd(Q,p) = Q/(mb)$ is always integer. The same is true for the second requirement in (25). Interestingly, this requirement is automatically satisfied by the MP combined winding. The reason is due to the constraint $\alpha_{\text{ph,w}} = 2\pi/m$, which reduces the effective number of phases in (21) depending on p and p_s and makes it possible that (24) is satisfied.

2) New requirements: In conventional MP machines, it is by default true that $\alpha_{\rm ph}$ cannot be a multiple of π (m>2). In MP combined windings, it must be also true that α_t and α_s are not multiples of π ($m_t>2$ and $m_s>2$). Based on the expressions from (20), these requirements are satisfied when p and p_s are not a multiple of m/2. This can be rewritten as:

$$\frac{2p}{m} \notin \mathbb{N}, \ \frac{2p_s}{m} \notin \mathbb{N} \tag{26}$$

All symmetry requirement are listed in Table I.

To show that (26) must be satisfied, the net torque and forces are now determined. Torque is calculated by substituting (15) into (4). Each torque phase current must be in phase with $T_{mt,k}$ to create the maximum torque per ampere:

$$i_{t,k} = I_t \cos\left(\theta + \pi/2 - p\alpha_{\text{w},k}\right) \tag{27}$$

Using complex numbers (phasors), (4) can be written as:

$$\tau = \frac{\hat{T}_{mt}I_t}{2}\Re\left\{\sum_{k=1}^m e^{j2\left(\theta + \frac{\pi}{2} - p\alpha_{w0} - [k-1]\alpha_t\right)} + m\right\}$$
(28)

If $\frac{2p}{m} \notin \mathbb{N}$ is satisfied, (28) simplifies to

$$\tau = k_t I_t, \ k_t = m\hat{T}_{mt}/2 \tag{29}$$

where k_t is a torque per ampere. However, if $\frac{2p}{m} \notin \mathbb{N}$ is not satisfied, the sum in (28) is not zero and the net torque is

$$\tau = 2k_t I_t \sin^2\left(\theta - p\alpha_{w0}\right) \tag{30}$$

where the torque has so-called "single-phase characteristics". The net force can be similarly determined. Each force phase current must be in phase with the $T_{md,k}$ term:

$$i_{x,k} = I_x \cos(\theta - p_s \alpha_{w,k}), \ i_{y,k} = \pm I_y \sin(\theta - p_s \alpha_{w,k})$$
$$i_{s,k} = i_{x,k} + i_{y,k} = I_s \cos(\theta - p_s \alpha_{w,k} \mp \phi)$$
(31)

where $I_s = \sqrt{I_x^2 + I_y^2}$, $\phi = \tan^{-1}(I_y/I_x)$ is a force angle, upper signs are for $p_s = h_1$ and lower signs are for $p_s = h_2$. The net force F_x is found in an analogous manner to (28):

$$F_x = \frac{I_x}{2} \left(\hat{T}_{mf,h1} \Re\{F_1 + F_2\} + \hat{T}_{mf,h2} \Re\{F_3 + F_4\} \right)$$
(32)

where F_1 and F_2 are the terms due to harmonic h_1 , and F_3 and F_4 are the terms due to harmonic h_2 :

$$F_1 = \sum_{k=1}^{m} e^{j(2\theta - [p_s + h_1]\alpha_{w,k})}, \ F_2 = \sum_{k=1}^{m} e^{j(p_s - h_1)\alpha_{w,k}}$$
(33)

$$F_3 = \sum_{k=1}^{m} e^{j(2\theta - [p_s + h_2]\alpha_{w,k})}, \ F_4 = \sum_{k=1}^{m} e^{j(p_s - h_2)\alpha_{w,k}}$$
(34)

If both $\frac{2p}{m} \notin \mathbb{N}$ and $\frac{2p_s}{m} \notin \mathbb{N}$ are satisfied, the force F_x is constant over all rotor angles (either F_2 or F_4 are non-zero):

$$F_x = k_f I_x, \ k_f = \frac{m\hat{T}_{mf,p_s}}{2}$$
 (35)

where k_f is a force per ampere. If $\frac{2p_s}{m} \notin \mathbb{N}$ is not satisfied, the force becomes $(F_1 \& F_2 \text{ or } F_3 \& F_4 \text{ are non-zero})$:

$$F_x = 2k_f I_s \cos^2\left(\theta - p_s \alpha_{w0}\right) \tag{36}$$

which has single-phase characteristics as in (30).

Finally, if $\frac{2p}{m} \notin \mathbb{N}$ is not satisfied, there is the effect of both harmonics $(F_2 \& F_3 \text{ or } F_1 \& F_4 \text{ are non-zero})$:

$$F_x = k_{f,h_{1/2}} I_x + k_{f,h_{2/1}} I_x \cos(2[\theta - p\alpha_{w0}])$$
 (37)

This case is acceptable only if single-phase torque characteristic is allowed and if k_{f,h_1} or k_{f,h_2} is zero.

D. Independent force/torque creation

Further restrictions are placed on the machine to ensure that the MP winding can independently control force and torque. This requires $T_{md}i_t=0$ and $T_{mt}i_s=0$. Using expressions developed for T_m matrix entries and the phase currents, the above constraint equations can be rewritten analogous to the equations (28) and (32) and used to determine conditions for independent force/torque creation. After doing these substitutions, it can be shown that the above constraints are satisfied if the following two constraints are met:

$$\sum_{k=1}^{m} e^{j(\alpha_s - \alpha_t)[k-1]} = 0 \tag{38}$$

$$\sum_{k=1}^{m} e^{j(2\theta - [\alpha_s + \alpha_t][k-1])} = 0$$
 (39)

TABLE I
MP COMBINED WINDING DESIGN REQUIREMENTS

Requirement	Standard	New
Symmetry	$z_c/m \in \mathbb{N}$	$2p/m \notin \mathbb{N}$
		$2p_s/m \notin \mathbb{N}$
Independent force/torque creation		$(p+p_s)/m \notin \mathbb{N}$

Condition (38) is always satisfied since $\alpha_s - \alpha_t = \pm 2\pi/m$. Condition (39) is violated only if $\alpha_s + \alpha_t$ is a multiple of 2π . In such case, (39) is equal to $me^{j2\theta}$, which results in a pulsating torque at 2θ due to force creating currents and a pulsating force at 2θ due to torque creating currents. Otherwise, if $\alpha_s + \alpha_t$ is not a multiple of 2π , (39) is always satisfied because the terms in the sum form a balanced set of vectors in a complex plane with a phase separation of $\frac{2\pi}{m}(p+p_s)$. Therefore, the following constraint ensures independent force/torque creation:

$$\frac{p+p_s}{m} \notin \mathbb{N} \tag{40}$$

This requirement is also listed in Table I (row 4 column 3).

E. Comparison of requirements to DPNV winding

This subsection compares the MP (Table I) and DPNV (Tables II-IV in [14]) combined winding design requirements. Although the windings create the same airgap fields, the power electronics implementation is different [21] and some design requirements are also different. The DPNV winding has more restrictions on the machine parameters than the MP combined winding. Designs that satisfy Table II-IV requirements in [14] also satisfy Table I requirements, but not vice versa. One reason is because the number of torque and suspension phases must be the same in the DPNV winding, which results in more restrictive symmetry requirements. The DPNV winding also requires no-voltage at the suspension terminals and nonzero suspension winding distribution factor k_{ds} to create force. In MP windings, k_{ds} can be made non-zero by adjusting the phase-slot assignment, resulting in more available combinations of slots, poles, and phases. However, some MP designs may have a decreased torque per ampere.

V. MP COMBINED WINDING DESIGN STEPS

Based on the requirements summarized in Table I, this section provides a design procedure to enable the designer to build a new bearingless machine with the MP combined winding or transform an existing motor design into a bearingless machine.

A. Design Steps

This subsection proposes a winding design approach using the torque and suspension star of slots diagrams. The design steps are now presented and then demonstrated later, for an example motor in Section V-B.

- 1) Select motor parameters that satisfy Table I requirements: Slots Q, pole pairs $(p \text{ and } p_s)$, and phases m.
- 2) Calculate torque and suspension phase angles: $\alpha_t = p\alpha_{\rm ph,w}$ and $\alpha_s = p_s\alpha_{\rm ph,w}$, with $\alpha_{\rm ph,w} = 2\pi/m$.
- 3) Draw torque and suspension star of slots diagrams: This is done similar to Fig. 2.

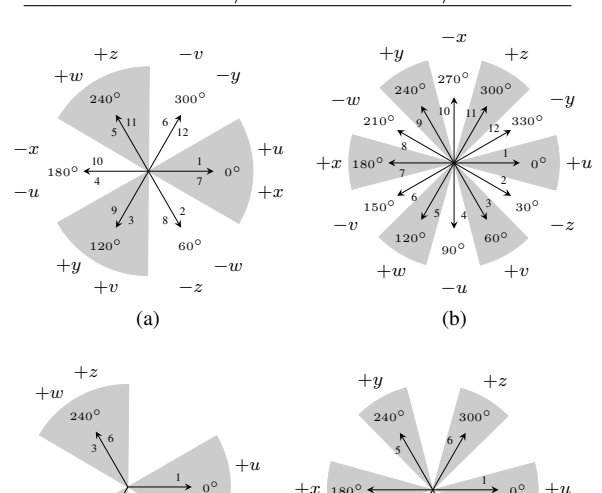
- 4) Assign each phase to one slot: Phase 1 to slot 1, phase 2 to slot 1+Q/m, ..., phase k to slot 1+(k-1)Q/m. This ensures that the angle between these slots is α_t and α_s in torque and suspension star of slots.
- 5) Assign phases to the remaining slots: There are Q-m remaining slots that have not been assigned to the phases. These slots must be selected so that the net phasor sum for each phase in both torque and suspension star of slots is not zero. If phase 1 is assigned to some slot X, then phase k is assigned to the slot number X+(k-1)Q/m. This guarantees that the resultant phasors have the phase separation α_t and α_s in torque and suspension star of slots. In fact, multiple winding design variants are possible in this step depending on the phase-slot assignment. These design variants differ from each other by different torque and suspension winding distribution factors k_{dt} and k_{ds} . The final design is selected based on the importance of torque creation vs. force creation. To maximize k_{dt} , the negative phase zone should be selected as close to 180° away from the positive zone as possible.
- 6) Select a coil span y: Select a coil span y to have non-zero torque and suspension winding factors k_{wt} and k_{ws} . This is ensured if the pitch factors are not zero. For harmonic h, the pitch factor is calculated as $k_{p,h} = \sin\left(h\frac{\alpha_y}{2}\right)$, where $\alpha_y = y\alpha_u$ is the coil pitch $(k_{pt}$ for torque and k_{ps} for suspension).
- 7) Pick p_s with higher k_{ws} : In some designs, both $p_s = p+1$ and p-1 can be symmetric. Therefore, p_s with a higher value of k_{ws} is selected for a final design.
- 8) Construct a winding diagram: Once all these steps are followed, the winding diagram can be constructed that shows the coil connections for each phase.

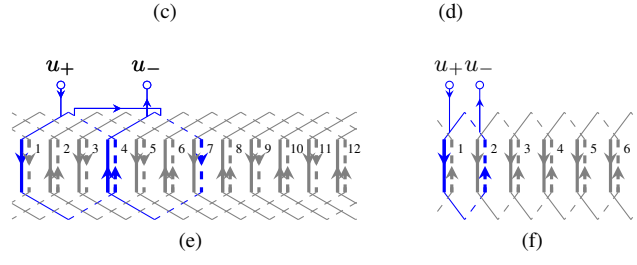
B. Example design

The proposed design steps are now demonstrated for a double-layer winding with $Q=12,\,p=2,\,p_s=1,$ and m=6:

- 1) From (23), $z_c = 12$; Table I design requirements are met.
- 2) $\alpha_{\rm ph,w} = \pi/3$, $\alpha_t = 2\pi/3$, and $\alpha_s = \pi/3$.
- 3) The diagrams are shown in Fig. 3a and 3b. The mechanical angle between adjacent slots is $\alpha_u = \pi/6$, resulting in $\pi/3$ in the torque and $\pi/6$ in the suspension star of slots.
- 4) The phases are labeled from u to z. They are assigned to the slots as follows: +u to 1, +v to 3, +w to 5, +x to 7, +y to 9, and +z to 11. The angle between these slots is α_t in torque star of slots and α_s in suspension star of slots.
- 5) The remaining slots (2, 4, 6, 8, 10, 12) are assigned to the phases to keep k_{dt} and k_{ds} non-zero. For the example motor, the possible phase assignment options are given in Table II. Among these variants, option 1 is selected (-u) to slot 4). Similarly, -v is assigned to slot 6, and so on (by an increment of Q/m=2). The resulting star of slots diagrams are shown in Fig. 3a and 3b.
- 6) The coil span is selected to ensure that both $k_{pt} = \sin\left(\frac{y\pi}{6}\right)$ and $k_{ps} = \sin\left(\frac{y\pi}{12}\right)$ are non-zero. For this example, y=3 so that $k_{pt}=1$ and $k_{ps}=0.707$. The resulting torque and suspension winding factors are $k_{wt}=1$ and $k_{ws}=0.5$.
- 7) $p_s = p + 1 = 3$ does not satisfy symmetry requirements. Therefore, $p_s = 1$ must be selected.

Assignment	k_{dt}/k_{ds}	Phase u phasor angle	
		(torque/susp. star of slots)	
-u to slot 4	1/0.707	0°/45°	
+u to slot 2	0.866/0.966	30°/15°	
+u to slot 6	0.866/0.259	330°/75°	





+y 120°

Fig. 3. Double-layer winding designs. $Q=12,\ m=6,\ p=2,\ p_s=1,$ and y=3: (a) torque star of slots; (b) suspension star of slots; and (e) winding layout. $Q=6,\ m=6,\ p=2,\ p_s=1,$ and y=1: (c) torque star of slots; (d) suspension star of slots; and (f) winding layout.

8) The resulting winding layout showing the connections for phase u is given in Fig. 3e.

The design procedure can similarly be used to design any MP combined windings satisfying the Table I requirements. A second example design with concentrated windings is given in Fig. 3f (with star of slots in Fig. 3c and 3d). For this design, the torque and suspension winding factors are 0.866 and 0.5. The phase separations of the phase currents must be $\alpha_t = 2\pi/3$ and $\alpha_s = \pi/3$ to independently create torque and force.

VI. VALIDATION OF MP COMBINED WINDING DESIGN

Validation of the MP combined winding design is now provided by studying the example winding designed in Fig. 3e. FEA has been conducted for the motor geometry shown in Fig. 4. This machine was designed for a rated speed of 30 kRPM and power of 25.5 kW, with 220 mm diameter and 100 mm axial length. The T_m matrix entries are calculated

using both FEA and (15)-(16). The machine is then excited with currents to create desired torque and force vectors. These results validate Sections III-V.

Figure 5a depicts the T_m matrix entries. The calculations of (15) and (16) approximately match the FEA tool calculations, which validates the results of Section III. As expected from (15), the $T_{mt,k}$ entries (row 3 in Fig. 5a) form a balanced system with $\alpha_t = 2\pi/3$ and $\hat{T}_{mt} = 0.58$ Nm. From (29), when each phase current is in phase with the corresponding $T_{mt,k}$ entry, the maximum torque per ampere is $k_t = 1.75$ Nm.

Interestingly, the $T_{mx,k}$ and $T_{my,k}$ entries (rows 1 and 2) do not form a balanced system (note the dissimilar amplitudes and phase separation). This is because each $T_{mx,k}$ and $T_{my,k}$ entry, according to (16), takes into account the effects of both $h_1 = p - 1 = 1$ and $h_2 = p + 1 = 2$ harmonics:

$$T_{mx,k} = 10.7\cos(\theta - h_1\alpha_{w,k}) + 7.8\cos(\theta - h_2\alpha_{w,k})$$
$$T_{my,k} = 10.7\sin(\theta - h_1\alpha_{w,k}) - 7.8\sin(\theta - h_2\alpha_{w,k})$$

For this example design, $\alpha_{w0,h_1}=0$ and $\alpha_{w0,h_2}=\pi$. Therefore, according to (10), $h_1\alpha_{w,k}=[k-1]\frac{\pi}{3}$ and $h_2\alpha_{w,k}=\pi+[k-1]\pi$ in the above equations. This shows that $T_{mx,k}$ (and $T_{my,k}$) terms consist of the sum of two balanced sets, one set having a phase separation $\pi/3$ and another set having π . If the phase separation $\alpha_s=\pi/3$ ($p_s=p-1$) between force creating phase currents i_s , multiplying T_m matrix in Fig. 5a by i_s results in the net constant force as in (35). In this case, there is no effect of the harmonic p+1 on the net force. However, if $\alpha_s=\pi$ ($p_s=p+1$), the net force would have single-phase characteristics as in (36). Therefore, $\alpha_s=\pi/3$ must be used to avoid asymmetry from harmonic p+1.

The proper operation of the example MP combined winding (if symmetry and independent force/torque creation are met) is now demonstrated using FEA simulation results for different force/torque commands. The first column of Fig. 5b shows that only torque is produced when currents are phase shifted by $\alpha_t = 2\pi/3$ (torque currents only), the second column shows that only force is produced when currents are phase shifted by $\alpha_s = \pi/3$ (force currents only), and the third column shows that both torque and force are produced when both currents are present (i_t and i_s). These forces and torque can also be determined by directly multiplying T_m matrix in Fig. 5a and the phase current waveforms.

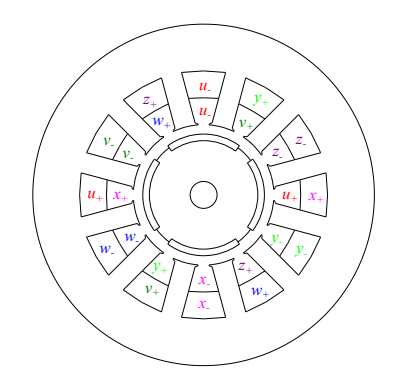


Fig. 4. Motor cross-section used with the MP winding design of Fig. 3e.

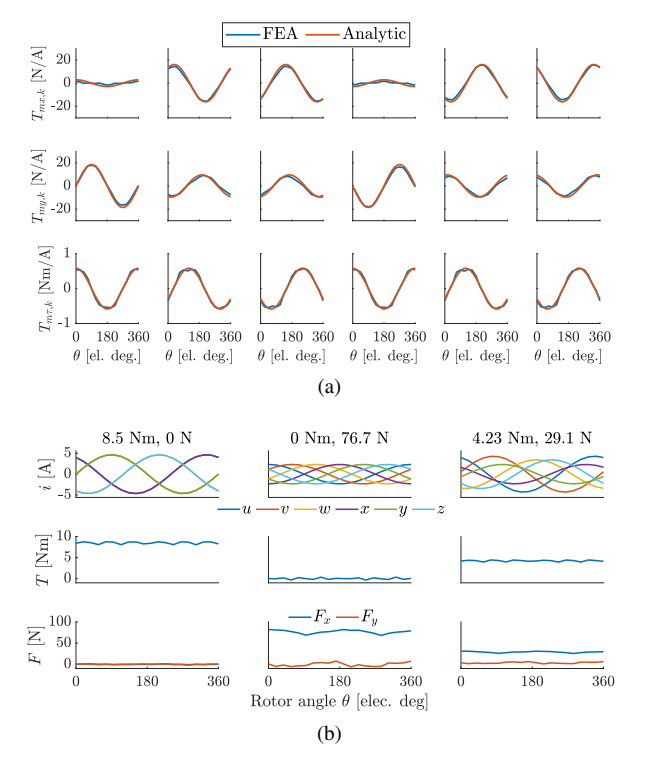


Fig. 5. FEA results for example MP winding design of Fig. 3e: (a) comparison of T_m matrix entries between FEA and analytic results and (b) calculated torque and force for different currents (column 1–rated torque, column 2–50% rated force, column 3–50% rated torque & 20% rated force).

VII. CONCLUSION

Historically, challenges in the winding design for bearingless motors have limited the machine performance (torque density, torque and force ripple, and efficiency). Combined windings are gaining attention as a potential solution for these problems, with MP combined windings being widely recognized as one of the highest performance approaches. This paper develops the fundamental force/torque model for machines employing these windings and uses this model to establish a winding analysis framework, machine design requirements, and a winding design procedure. While it is found that many combinations of stator slots, poles, and phases can lead to viable windings, certain combinations lead to either asymmetric windings or cross-coupling between the motor and suspension operation. It is also found that the classical star of slots design methodology for stator windings can be extended to aid in the design of MP combined windings by considering both the motor and suspension field spatial harmonics.

Motor designers will find this paper useful as a practical guide to rapidly design MP combined windings for various slot-pole combination motors. The goal of this paper is to help the research community develop more compact, efficient, precise, and lower cost bearingless motors, thereby allowing this technology to reach into application spaces where magnetic levitation has historically not been successful.

REFERENCES

 A. Chiba, T. Fukao, O. Ichikawa, M. Oshima, M. Takemoto, and D. Dorrell, Magnetic Bearings and Bearingless Drives. Newnes, 2005.

- [2] S. Silber, W. Amrhein, P. Bosch, R. Schob, and N. Barletta, "Design aspects of bearingless slice motors," *IEEE/ASME Transactions on Mechatronics*, vol. 10, no. 6, pp. 611–617, Dec 2005.
- [3] D. Dietz and A. Binder, "Comparison between a bearingless pm motor with separated and combined winding for torque and lateral force generation," in 2019 21st European Conference on Power Electronics and Applications (EPE'19 ECCE Europe). IEEE, 2019, pp. P-1.
- [4] W. Gruber, T. Nussbaumer, H. Grabner, and W. Amrhein, "Wide air gap and large-scale bearingless segment motor with six stator elements," *IEEE Transactions on Magnetics*, vol. 46, no. 6, pp. 2438–2441, 2010.
- [5] S. Silber and W. Amrhein, "Power optimal current control scheme for bearingless pm motors," in *Proc. 7th Int. Symp. Magn. Bearings*, 2000, pp. 401–406.
- [6] Min Kang, Jin Huang, Hai-bo Jiang, and Jia-qiang Yang, "Principle and simulation of a 5-phase bearingless permanent magnet-type synchronous motor," in 2008 International Conference on Electrical Machines and Systems, 2008, pp. 1148–1152.
- [7] V. F. Victor, J. de Paiva, A. O. Salazar, and A. L. Maitelli, "Performance analysis of a neural flux observer for a bearingless induction machine with divided windings," in 2009 Brazilian Power Electronics Conference, 2009, pp. 498–504.
- [8] W. K. S. Khoo, "Bridge configured winding for polyphase self-bearing machines," *IEEE Transactions on Magnetics*, vol. 41, no. 4, pp. 1289– 1295, 2005.
- [9] R. Oishi, S. Horima, H. Sugimoto, and A. Chiba, "A novel parallel motor winding structure for bearingless motors," *Magnetics, IEEE Transactions* on, vol. 49, no. 5, pp. 2287–2290, 2013.
- [10] E. Severson, S. Gandikota, and N. Mohan, "Practical implementation of dual-purpose no-voltage drives for bearingless motors," *IEEE Transactions on Industry Applications*, vol. 52, no. 2, pp. 1509–1518, March 2016.
- [11] G. Valente, A. Formentini, L. Papini, P. Zanchetta, and C. Gerada, "Position control study of a bearingless multi-sector permanent magnet machine," in *IECON* 2017 - 43rd Annual Conference of the *IEEE* Industrial Electronics Society, 2017, pp. 8808–8813.
- [12] A. Chiba, K. Sotome, Y. Iiyama, and M. Azizur Rahman, "A novel middle-point-current-injection-type bearingless pm synchronous motor for vibration suppression," *Industry Applications, IEEE Transactions on*, vol. 47, no. 4, pp. 1700–1706, 2011.
- [13] W. Gruber and S. Silber, "Dual field-oriented control of bearingless motors with combined winding system," in 2018 International Power Electronics Conference (IPEC-Niigata 2018 -ECCE Asia), May 2018, pp. 4028–4033.
- [14] E. L. Severson, R. Nilssen, T. Undeland, and N. Mohan, "Design of dual purpose no-voltage combined windings for bearingless motors," *IEEE Transactions on Industry Applications*, vol. 53, no. 5, pp. 4368–4379, 2017.
- [15] J. Pyrhonen, T. Jokinen, and V. Hrabovcova, Design of rotating electrical machines. John Wiley & Sons, 2013.
- [16] S. Rubino, O. Dordevic, E. Armando, R. Bojoi, and E. Levi, "A novel matrix transformation for decoupled control of modular multiphase pmsm drives," *IEEE Transactions on Power Electronics*, 2020.
- [17] E. Levi, M. Jones, S. N. Vukosavic, and H. A. Toliyat, "A novel concept of a multiphase, multimotor vector controlled drive system supplied from a single voltage source inverter," *IEEE transactions on Power Electronics*, vol. 19, no. 2, pp. 320–335, 2004.
- [18] E. Levi, R. Bojoi, F. Profumo, H. Toliyat, and S. Williamson, "Multiphase induction motor drives—a technology status review," *IET Electric Power Applications*, vol. 1, no. 4, pp. 489–516, 2007.
- [19] G. Sala, M. Mengoni, G. Rizzoli, L. Zarri, and A. Tani, "Decoupled d-q axes current-sharing control of multi-three-phase induction machines," *IEEE Transactions on Industrial Electronics*, vol. 67, no. 9, pp. 7124– 7134, 2019.
- [20] E. Levi, "Advances in converter control and innovative exploitation of additional degrees of freedom for multiphase machines," *IEEE Transactions on Industrial Electronics*, vol. 63, no. 1, pp. 433–448, 2015.
- [21] A. Khamitov, W. Gruber, G. Bramerdorfer, and E. L. Severson, "Comparison of combined winding strategies for radial non-salient bearingless machines," *IEEE Transactions on Industry Applications*, pp. 1–1, 2021.
- [22] J. Chen, J. Zhu, and E. L. Severson, "Review of bearingless motor technology for significant power applications," *IEEE Transactions on Industry Applications*, vol. 56, no. 2, pp. 1377–1388, 2020.